Inorg. Chem. **2008**, *47*, 7623−7630

Synthesis and Magnetic Properties of New Mono- and Binuclear Iron Complexes with Salicyloylhydrazono Dithiolane Ligand

Nouri Bouslimani,[†] Nicolas Clément,[†] Guillaume Rogez,[‡] Philippe Turek,[§] Maxime Bernard,[§] Samuel Dagorne,[†] David Martel,[||] Hoan Nguyen Cong,[||] and Richard Welter*[,†]

Laboratoire DECOMET, UMR 7177 CNRS, Université Louis Pasteur, 4, rue Blaise Pascal, 67070 Strasbourg Cedex, France, I.P.C.M.S., UMR 7504 CNRS-ULP, Groupe des Materiaux Inorganiques, 23 Rue du Loess, BP 43, F-67034 Strasbourg Cedex 2, France, Laboratoire POMAM, UMR 7177 CNRS, Université Louis Pasteur, 1, rue Blaise Pascal, BP 296 R8, 67008 Strasbourg Cedex, France, and Laboratoire d'Electrochimie et de Chimie Physique du Corps Solide, UMR 7177 CNRS-ULP, Université Louis Pasteur Strasbourg I, F-67070 Strasbourg cedex, France

Received March 22, 2008

We report here experimental evidence for the formation in the solid state of a new binuclear $Fe^{III}_2(\mu\text{-}OMe)_2(HL)_4$ complex (H_2L is 2-salicyloylhydrazono-1,3-dithiolane). The isostructural $Mn^{III}_2(\mu\text{-}OMe)_2(HL)_4$ complex has provided the strongest ferromagnetic interaction value ($J \approx 20$ cm^{-1}) between Mn^{III} ions to date. The new iron binuclear compound presented in this study shows antiferromagnetic intramolecular coupling, which agrees with the theoretical study that we previously proposed. During our synthetic work, we also observed an unexpected spontaneous reduction of the new $Fe^{III}(HL)_2Cl,S$ complex to the new $Fe^{II}(H_2L)_2Cl_2$ high-spin mononuclear complex. This process has been checked by cyclo-voltammetry as well as pseudosteady voltammetry.

Introduction

The control of exchange magnetic coupling at the molecular scale is one of the most challenging themes in the field of molecular magnetism. Among a large variety of magnetically interesting molecules,[1] special attention has been paid to exchange coupled clusters (ECC). An ECC molecule typically consists of a small number (∼4 to 30) of paramagnetic transition-metal ions, which are linked together by simple bridges such as O^{2-}, HO^-, CH_3O^-, F^-, Cl^-, $RCOO^-$. The bridges provide a superexchange pathway, giving rise to an isotropic coupling on the order of 1 to 100 cm^{-1}. Some ECC show slow relaxation of magnetization of purely molecular origin and they are usually called single molecule magnets (SMM).[2−5] Probably, the most famous example is $[Mn_{12}O_{12}(CH_3COO)_{16}(H_2O)_4]$ ($[Mn_{12}(OAc)]$)[5,6] that still remains a golden standard due to combination of a large spin state ($S = 10$) and negative zero-field splitting axial parameter ($D = -0.5$ cm^{-1}). A record value for the energy barrier to magnetization reversal of SMM was reported recently for a hexanuclear Mn^{III} compound ($S = 12$, $D = -0.43$ cm^{-1}, $U_{eff} = 86.4$ K).[7] Although the feasibility of SMM for technological application in information storage or quantum computing[8] is still quite questionable (especially in view of the recent findings[9]), studies of SMM contribute to an understanding of magnetic phenomena such as, for instance, quantum tunnelling of the magnetization. On the other hand, ECC with lower nuclearity are versatile building blocks for cooperatively associated magnetic systems.[10] They can also be incorporated in crystal lattices together with

* Author to whom correspondence should be addressed. E-mail: welter@chimie.u-strasbg.fr, Tel: +33 90 24 15 93, Fax: +33 90 24 12 29.
[†] Laboratoire DECOMET, Université Louis Pasteur.
[‡] I.P.C.M.S., Groupe des Materiaux Inorganiques.
[§] Laboratoire POMAM, Université Louis Pasteur.
[||] Laboratoire d'Electrochimie et de Chimie Physique du Corps Solide, Université Louis Pasteur Strasbourg I.

(1) Kahn, O., *Molecular Magnetism*; Wiley-VCH: New York, 1993.
(2) Single-Molecule Magnets and Related Phenomena. In *Structure Bonding*; Winpenny, R., Ed.; Berlin, 2006; *122*.
(3) Sessoli, R. *Mol. Cryst. Liq. Cryst.* **1995**, *274*, 145.
(4) Gatteschi, D.; Sessoli, R. *Angew. Chem., Int. Ed.* **2003**, *42*, 268.
(5) Caneschi, A.; Gatteschi, D.; Sessoli, R. *J. Am. Chem. Soc.* **1991**, *113*, 5873.
(6) Lis, T. *Acta Crystallogr.* **1980**, *B36*, 2042.
(7) Milios, C. J.; Vinslava, A.; Wernsdorfer, W.; Moggach, S.; Parsons, S.; Perlepes, S. P.; Christou, G.; Brechin, E. K. *J. Am. Chem. Soc.* **2007**, *129*, 2754–2755.
(8) Leuenberger, M. N.; Loss, D. *Nature,* **2001**, *410*, 789.
(9) Ruiz, E.; Cirera, J.; Cano, J.; Alvarez, S.; Loose, C.; Kortus, J. *Chem. Commun.* **2008**, 52.

10.1021/ic800522h CCC: $40.75
Published on Web 07/29/2008

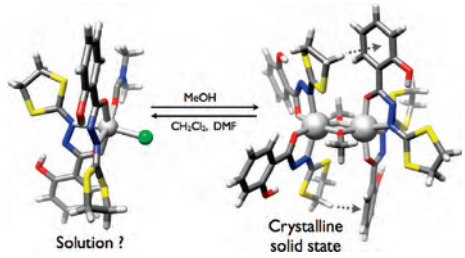

Figure 1. Hypothetical situation between paramagnetic T^{III} mononuclear and binuclear complexes.

conducting molecules, leading to innovative magnetic/conducting bifunctional materials.[11] Because of the dependence of the coupling pathways on structure and symmetry of the organic ligands, dinuclear ECC offer interesting possibilities to tune metal-to-metal interactions by small structural changes of the organic periphery. Following this approach, we have been working on small modifications of the organic periphery as well as the metallic centers of a very exciting dinuclear Mn^{III} complex $[Mn_2(\mathbf{HL})_4(\mu\text{-}OCH_3)_2]$ (where $\mathbf{H_2L}$ is 2-salicyloylhydrazono-1,3-dithiolane), which present the largest J value ($J = +19.7$ cm^{-1}) ever reported so far for a $Mn^{III}-Mn^{III}$ interaction.[12] The peculiarity of the $[Mn_2(\mathbf{HL})_4(\mu\text{-}OCH_3)_2]$ structure (in the solid state) is an unsymmetrical arrangement of the ligands that is responsible for ferromagnetic ground state.[12] This unexpected situation has to be related to intramolecular nonclassical hydrogen bonds occurring between hydrogen atoms of the dithiolane ring and the centroid of the phenol groups (Figure 1). In the present article, we specifically focus on iron compounds obtained with the same H_2L ligand to investigate in solution (with the use of EPR studies) the equilibrium between mono- and binuclear complexes.

Results and Discussion

Ligand $\mathbf{H_2L}$ was prepared as previously reported where $\mathbf{H_2L}$ is 2-salicyloylhydrazono-1,3-dithiolane).[13,14] The first step in the present work was to examine the possibility to obtain well-defined molecular complexes when the ligand $\mathbf{H_2L}$ is reacted with Fe^{III} salts. Considering the results described hereafter, commercial crystalline $FeCl_3$ and/or $Fe(acac)_3$ have been selected as main-metal sources.

The reaction of the ligand $\mathbf{H_2L}$ (2 equiv) with iron(III) chloride in DMF as solvent affords **C1** (step A, Scheme 1) in a good yield. Dark-blue single crystals have been obtained by diffusion of diethyl ether into the DMF solution of the complex under air. When the recrystallization process was performed in sealed glass tubes, we observed the formation of a yellow complex **C2** (step F′, Scheme 1), which was

Scheme 1. Synthesis of **C1**, **C2**, and **C3** from $\mathbf{H_2L}$

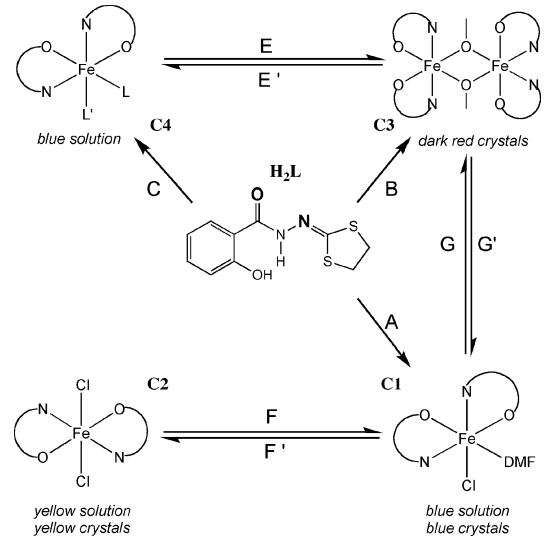

isolated as air-sensitive single crystals after a slow diffusion of diethyl ether into the DMF solution (Figure 2).

The solvation of the single crystals of **C2** by DMF solvent (under air) gives back, instantly, a blue solution of **C1** (step F, Scheme 1). In addition, these yellow crystals of **C2**, as they are air-sensitive, were found to slowly convert (within a few days) to blue solid under air exposure. A similar observation has been done with a DMF solution of **C2** (under stirring), which can be quickly (within few seconds) oxidized to **C1** under air exposure.

From electrochemical studies as well as EPR, magnetic measurements, and crystal-structures determination, we can assume that the iron atoms in **C1** are in a (+III) oxidation state, both in solution and in crystals, whereas those in **C2** are in a (+II) oxidation state. A preliminary study of this unusual spontaneous reduction of Fe^{III} to Fe^{II} was carried out by electrochemical investigations (Figures 11 and 12).

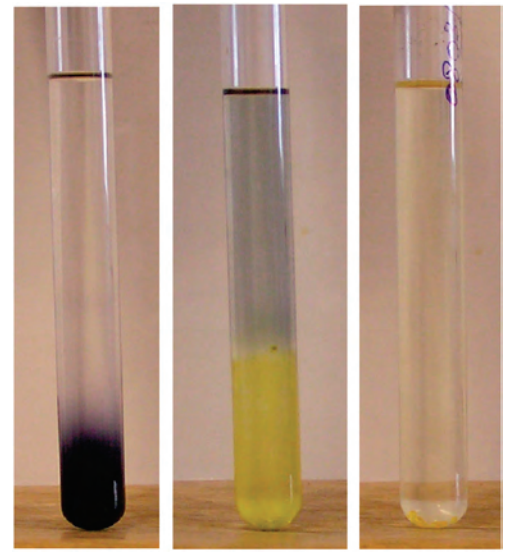

Figure 2. Left, starting point of the diffusion process of diethyl ether (colorless liquid) in **C3** solution (blue, in DMF); middle, color change (blue to yellow) when the diethyl ether diffuses in the DMF solution; right, end of the diffusion process with the yellow crystals on the glass tube bottom.

(10) Ferbinteanu, M.; Miyasaka, H.; Wernsdorfer, W.; Nakata, K.; Sugiura, K. I.; Yamashita, M.; Coulon, C.; Clérac, R. *J. Am. Chem. Soc.* **2005**, *127*, 3090.
(11) Hiraga, H.; Miysaka, H.; Nakata, K.; Kajiwara, T.; Takaishi, T.; Oshima, Y.; Nojiri, H.; Yamashita, M. *Inorg. Chem.* **2007**, *46*, 9661.
(12) Beghidja, C.; Rogez, G.; Kortus, J.; Wesolek, M.; Welter, R. *J. Am. Chem. Soc.* **2006**, *128*, 3140.
(13) Beghidja, C.; Wesolek, M.; Welter, R. *Inorg. Chim. Acta* **2005**, *358*, 3881.
(14) Chen, H. C.; Gong, X. Q.; Luo, J. X.; Huang, F.; Fang, J. Y.; Pan, Z. J.; Liu, W. J. *Chin. J. Org. Chem.* **2000**, *5*, 833.

Nevertheless, the actual mechanism of this reduction process is not yet well understood as of today.

Single crystals of **C2** were obtained in numerous solvent/nonsolvent conditions (Experimental Section). These three refined crystal structures are given as Supporting Information (CIF files, hydrogen bonds, tables), and their compared description is given hereafter.

The binuclear Fe^{III} **C3** could be prepared by two methods depending on the Fe^{III} salt used for the preparation. The direct reaction of the ligand $\mathbf{H_2L}$ with $FeCl_3$ in methanol in the presence of sodium acetate (AcONa) (step B, Scheme 1) yields a dark-red polycrystalline powder of **C3**, which can be recrystallized from a THF solution by slow diffusion of methanol to afford well-formed dark-red crystals of **C3**. Likewise, the reaction of the ligand $\mathbf{H_2L}$ with $Fe(acac)_3$ in DMF or THF (step C, Scheme 1) affords the hypothetical (nonisolated) mononuclear species **C4**, which can be considered as an intermediate in the formation of **C3** as evidenced by EPR spectroscopy (L, L′ are the remaining acetylacetonate ligand from step C, or the methoxy group and a solvent ligand resulting from the solvation of **C3** in the step E′). Slow diffusion of methanol into a THF solution of **C4** (step E, Scheme 1) gave dark-red crystals of **C3**. An alternative method can be used for the preparation of **C3** starting from the mononuclear **C1** (which can also be considered as an intermediate in the formation of **C3**) by addition of sodium acetate to a methanol solution of **C1** (step G, Scheme 1). Finally, in light of what was explained above, the hypothetical situation between **C1** and **C3** (step G′ Scheme 1) can be rationalized. Moreover, we succeeded in synthesizing the complex **C2** from direct reaction of H_2L and $FeCl_2$ in DMF. This procedure led to the rapid formation of a yellow solution of **C2**, which was isolated and characterized as yellow single crystals (obtained by diethyl ether diffusion in DMF).

These three iron paramagnetic complexes (**C1**, **C2** and **C3**) have been completely characterized by single-crystal diffraction.

Description of the Crystal Structures. NB: Crystallographic data (as well as full hydrogen bonding scheme) are gathered in the Supporting Information, and the selected bond lengths and angles are given in the corresponding figure captions (Figures 3, 4 and 5).

C1 crystallizes in the monoclinic space group $P2_1/c$. As clearly shown in Figure 3, both $\mathbf{HL}^-$ ligands around the Fe^{III} cation remain planar and are in a cis configuration, as already observed for the analogous Mn^{II}[13] or Mn^{III}[12] complexes. The octahedral coordination environment of the Fe^{III} ion in **C1** is classical and includes a chloride atom and one DMF molecule. Three intramolecular hydrogen bonds are detected[15] and are located between O1 and N1 via H1O, O3, and N3 via H3O and at least between O5 and C22 via H22C. From the crystal packing point of view, a 3D arrangement is observed, the packing being related to numerous van der Waals contacts.

Single crystals of **C2** have been obtained as described above (also Figure 2). This compound crystallizes in the triclinic centrosymmetric space group $P\bar{1}$. As shown in Figure 4, the compound consists of a mononuclear complex of iron(+II). The presence of hydrogen atoms on the N1 and N3 nitrogen atoms (clearly pointed out by Fourier differences and by the special conformation of the hydroxyl groups) indicates that both bidentate ligands are neutral. Considering both chloride atoms (−I) to complete the octahedral surrounding of the iron cation, it is in +II oxidation state. This is confirmed by solid-state EPR as well as by magnetometric measurements (Curie constant $C = 3.68$ emu·K·mol^{-1}, in perfect agreement with a high-spin Fe^{II} complex, Figure S4 in the Supporting Information). In **C2**, both bidendate $\mathbf{H_2L}$ ligands are in a trans configuration, as observed in the analogous $Mn^{+II}(HL)_2(Py)_2$ compounds.[13]

Twelve hydrogen bonds have been detected in the crystal structure of **C2**(Et_2O); these most likely account for the great stability of this Fe^{II} compound in the solid state. The large Fe−N, Fe−O and Fe−Cl bond distances deduced from the diffraction data (Figures 4, 5 and 6) are in accordance with a high-spin electronic configuration ($S = 2$) for this complex. Nevertheless, the formation of **C2** from **C1** remains unclear to us: it constitutes, to the best of our knowledge, the first example of spontaneous reduction in solution of a high spin

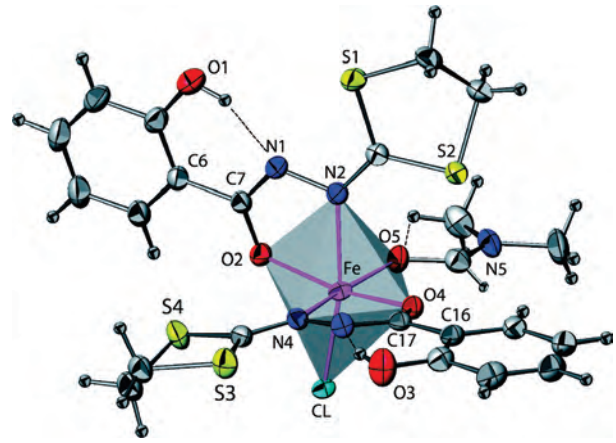

Figure 3. *ORTEP* view of **C1** with partial labeling scheme. The ellipsoids enclose 50% of the electronic density. The dashed lines show intramolecular hydrogen bonds. Selected bonds length (angstroms) and angles (degrees): Fe−O2, 1.973(4); Fe−O4, 1.977(4); Fe−O5, 2.035(4); Fe−N4, 2.145(5); Fe−N2, 2.213(5); Fe−Cl, 2.3318(14); O2−Fe−O4, 159.84(17); O5−Fe−N4, 166.56(17).

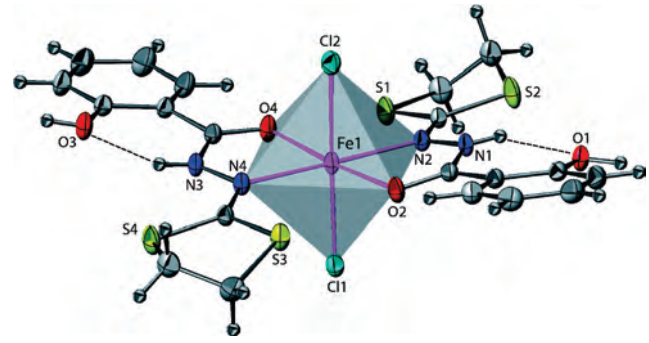

Figure 4. *ORTEP* view of **C2**(Et_2O) with partial labeling scheme. The ellipsoids enclose 50% of the electronic density. The Et_2O solvent molecule is omitted for clarity. The dashed lines show intramolecular hydrogen bonds. Selected bonds length (angstroms) and angles (degrees): Fe1−O2, 2.115(1); Fe1−O4, 2.122(1); Fe1−N4, 2.199(1); Fe1−N2, 2.229(1), Fe1−Cl1 2.4396(7), Fe1−Cl2 2.4613(7); O2−Fe1−O4, 175.41(4); O4−Fe1−N4, 74.55(4).

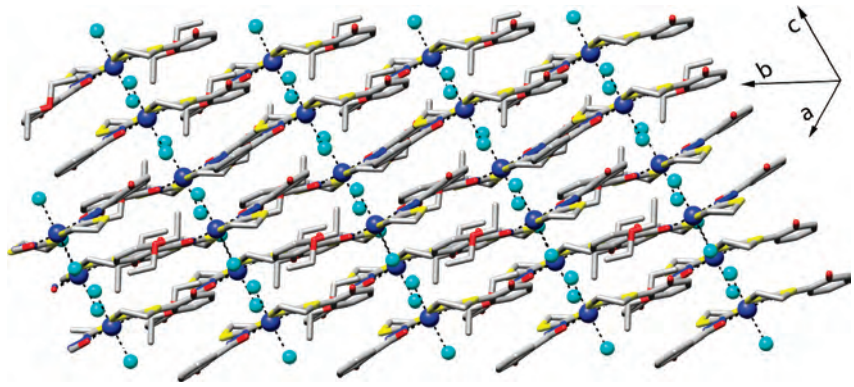

Figure 5. Partial view[17] of the crystal packing in complex **C2**(Et_2O). The hydrogen atoms are omitted for clarity. The dashed lines represent the Cl1−Fe1−Cl2 bonds.

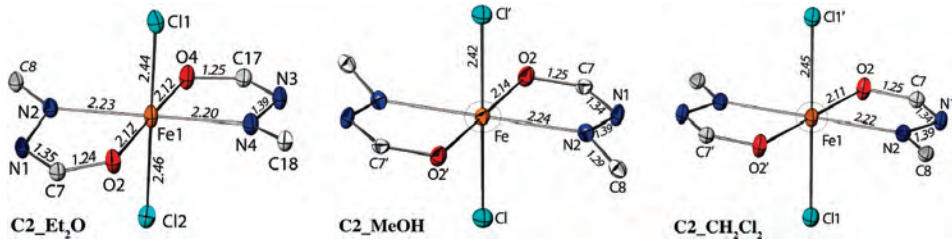

Figure 6. Structural comparison of the three refined crystal structures of the **C2** complexes. Only the direct iron coordination sphere is represented with bond labels. The circles around the Fe^{II} atoms (**C2**_$(MeOH)_2$ and **C2**_$(CH_2Cl_2)_2$) indicate symmetry centers. Symmetry operator for equivalent positions: $-x + 2, -y, -z + 1$.

Fe^{III} complex to a high spin Fe^{II} complex (one related case can be found in ref 16), well characterized in the solid state. A packing view of **C1** in the solid state is given in Figure 5. The structure can be described as a pseudo-bidimensionnal arrangement of complex **C2**(Et_2O) (all Cl1−Fe1−Cl2 axes are aligned), the molecules being connected to each other by hydrogen bonds (Table S2 in the Supporting Information) and/or van der Waals contacts.

Crystals of **C2** can also be obtained from THF solution of $FeCl_3$ and 2 equiv of the ligand **H2L** by slow diffusion of methanol and from ethanol solution of the same mixture by slow diffusion of CH_2Cl_2. In both cases, well-formed yellow crystals of **C2** (named **C2**_methanol and **C2**_dichlo) are obtained and characterized. The three different crystal structures of **C2** can be compared regarding the following points:

• The lattice symmetry is monoclinic for **C2**_MeOH and **C2**_CH_2Cl_2, whereas this symmetry is triclinic for **C2**(Et_2O). Moreover, in this last case, there is no symmetry center on the iron atom.

• By changing the crystallization conditions, different solvent molecules are incorporated in the crystal lattice: one Et_2O molecule for **C2**(Et_2O) per iron complex, two MeOH and two CH_2Cl_2 per iron complex for **C2**_methanol and **C2**_dichlo, respectively.

• Finally, the molecular cores of the three compounds are very similar (distances and angles are the same), as clearly shown in Figure 6, which confirm the +II oxidation and high-spin state of the iron ion in these **C2** complexes.

C3, obtained as well-formed dark-red single crystals, crystallizes in the monoclinic centrosymmetric space group $P2_1/n$. This compound consists of a μ-methoxo binuclear Fe^{III} complex, as expected. The molecular structure (Figure 7) can be described as a neutral asymmetric complex, where each iron ion is chelated by two HL^- bidentate ligands and bridged by two methoxy anions.

As already observed for the analogous Mn^{III} compound, **C3** features a nonsymmetrical situation for the two metal ions. In fact, Fe1 and Fe2 are in two different distorted octahedra. Around Fe1, both nitrogen atoms N2−N4 are in a trans configuration, and around Fe2 both nitrogen atoms N6−N8 are in a cis configuration. From another point of view, the four oxygen atoms are quite square-planar around Fe1, whereas the four oxygen atoms are in tetrahedral configuration around Fe2. This special situation is related to both nonclassical intramolecular hydrogen bonds found between C10 and the centroid of the C31_C36 phenol group and C20 and the centroid of the C21_C26 phenol group (Figure 5). It is important to note that this μ-methoxo binuclear iron compound adopts the same molecular structure and the same crystal symmetry as that previously described for the analoguous Mn^{III} complex.[12] From a crystal packing point of view, a 3D arrangement is observed, the packing being related to numerous hydrogen bonds as well as van der Waals contacts (Table S2 in the Supporting Information). With two additional electrons for this complex versus its manganese analogue ($Mn^{III} \rightarrow Fe^{III}$), it is of course highly relevant to analyze the magnetic properties of this new complex.

Magnetic Measurements of the μ-Methoxo Binuclear Iron C3. The magnetic properties of the **C3** μ-methoxo binuclear iron(III) complex were investigated in the solid state in the 300−1.8 K temperature range with an applied field of 5 kOe (Figure 8). The χT value at room temperature (5.74 emu·K·mol^{-1}) is well below the expected value for two high-spin Fe^{III} (8.75 emu·K·mol^{-1} assuming $g = 2$).

Upon cooling, the χT product decreases continuously, down to almost 0 (0.05 emu·K·mol^{-1} at 1.8 K). This indicates the occurrence of a relatively strong antiferromagnetic intramolecular interaction between the two Fe^{III} ions, which is in perfect accordance with the orbital model previously described for the analogous Mn^{III} dimer.[12] In the present case, all orbitals are half-filled, and thus the ferromagnetic pathways resulting from the interaction between one half-filled and one empty orbitals are no longer available.

The data were fitted using the following spin Hamiltonian where all parameters have their usual meaning and the spin operator **S** is defined as $\boldsymbol{S} = \boldsymbol{S}_{\mathbf{Fe1}} + \boldsymbol{S}_{\mathbf{Fe2}}$:

$$H = -J\boldsymbol{S}_{\mathbf{Fe1}}\boldsymbol{S}_{\mathbf{Fe2}} + g\beta HS$$

To reproduce the data satisfactorily we had to consider a certain amount ρ of paramagnetic impurity ($\boldsymbol{S}_{\mathbf{impur}} = {}^5/_2$). The fit leads the following values: $J = -27.4(1)$ cm^{-1}, $g = 2.05(1)$, and $\rho = 0.79(1)$ % with an excellent agreement factor $R = 7.6 \times 10^{-5}$ (R is defined as $R = \sum(\chi_{exptl} - \chi_{calcd})/\sum \chi^2_{exptl}$).

The value of exchange coupling constant determined for **C3**(MeOH)$_2$ is perfectly in line with the values reported for other symmetric bis-μ-alkoxo bridged diiron(III) complexes with similar structural features (Fe−Fe distances and Fe−O−Fe angles).[18]

Despite many attempts, it is very difficult to give a general tendency for an accurate magneto-structural correlation for weakly coupled Fe^{III} binuclear complexes. Although it is clear that some parameters (the Fe−Fe distance, the Fe−O−Fe angle) play a role, their relative contribution to the coupling constant J is still questioned. As an example, the very nice correlation established by Le Gall et al. between J and the Fe−O−Fe angle for a family of binuclear Fe^{III} complexes with β-diketonate-alkoxide peripheral ligands[19] does not apply to all the other complexes reviewed for instance by R. Werner et al.[18] The semiempirical relation established by Gorun and Lippard[20] is probably the best compromise between simplicity and accuracy. It gives J as a function of a coupling distance P, defined as half the shortest superexchange pathway between the two Fe^{III} ions:

$J = A \exp(B \times P)$ (referring to the following Hamiltonian: $H = -J\boldsymbol{S}_{\mathbf{Fe1}}\boldsymbol{S}_{\mathbf{Fe2}}$)

The parameters reported by Gorun and Lippard[20] have been refined by R. Werner et al.[18] who have reported $A = -2.16 \times 10^{13}$ cm^{-1} and $B = -13.9$ Å^{-1}.

For the present-studied complex **C3**(MeOH)$_2$, $P = 1.977$ Å, this semiempirical formula gives $J = -25.1$ cm^{-1}, in very good agreement with the experimental value.

(15) Spek, A. L. *PLATON, J. Appl. Crystallogr.* **2003**, *36*, 7.
(16) Patra, A. K.; Olmstead, M. M.; Mascharak, P. K. *Inorg. Chem.* **2002**, *41*, 5403.
(17) Pettersen, E. F.; Goddard, T. D.; Huang, C. C.; Couch, G. S.; Greenblatt, D. M.; Meng, E. C.; Ferrin, T. E. *J. Comput. Chem.* **2004**, *25*, 1605.
(18) Werner, R.; Ostrovsky, S.; Griesar, K.; Haase, W. *Inorg. Chim. Acta* **2001**, *326*, 78.
(19) Le Gall, F.; Biani, F. F.; Caneschi, A.; Cinelli, P.; Cornia, A.; Fabretti, A. C.; Gatteschi, D. *Inorg. Chim. Acta* **1997**, *262*, 123.
(20) Gorun, S. M.; Lippard, S. J. *Inorg. Chem.* **1991**, *30*, 1625.

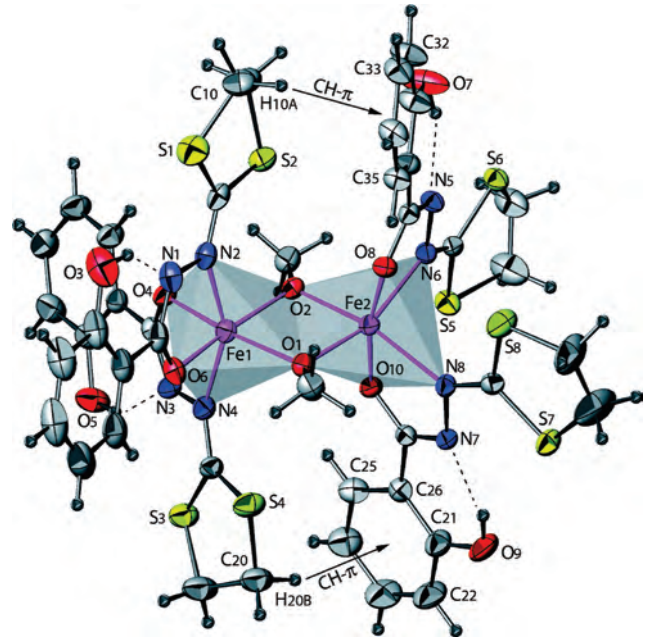

Figure 7. *ORTEP* view of **C3**(MeOH)$_2$ with partial labeling scheme. The ellipsoids enclose 50% of the electronic density. Both MeOH solvent molecules are omitted for clarity. The dashed lines show representative intramolecular hydrogen bonds and the arrows represent the CH−π interactions. Selected bonds length (angstroms) and angles (degrees): Fe1−O2, 1.974(2); Fe1−O4, 1.966(2); Fe2−O1, 1.967(2); Fe2−O8, 1.964(2); Fe1−N2, 2.173(3); Fe1−N4, 2.173(3); Fe2−N6, 2.150(3); Fe2−N8, 2.171(3); Fe1−Fe2,, 3.085(4).

EPR Studies of the μ-Methoxo Binuclear Iron Complex C3. The EPR spectra of the compound **C3** have been recorded at different temperatures both in frozen solution and in the solid state for polycrystalline powders. The EPR signal of powders is temperature dependent, both in shape and in intensity (Figure 9). It corresponds to a high-spin hexacoordinated Fe^{III} ion at 4 K with a rhombic g-tensor: $g_1 = 8.28$, $g_2 = 4.38$, $g_3 = 2.07$.[21] As the temperature increases, extra lines superimpose to this base signal, which intensity decreases. Considering these spectra parallel to the static magnetic behavior, the low-temperature features should be attributed to isolated monomer impurities as evidenced by the Curie tail in the SQUID susceptibility (Figure 8).

Starting from the nonmagnetic ground state ($S = 0$) where only Curie impurities are observed, higher-spin multiplets are thermally populated and the additional features should be ascribed to these multiplets. A detailed study of these fine structure lines has not been performed in the explored X-band frequency range because a higher frequency is more relevant for such investigation.

The compound is EPR silent in fluid solution at room temperature. The EPR signal in frozen solution exhibits hyperfine structure superimposed to the signal of an isolated high-spin hexacoordinated Fe^{III} ion throughout the studied temperature range (4−100 K). This high-spin Fe^{III} spectrum has a similar g tensor than the one observed at 4 K for the powder (Figure 10). The hyperfine pattern is ascribed to the four nonequivalent ^{14}N nuclei directly bound to the iron ions. The broadening of the hyperfine lines makes them disappear as the temperature increases. Unlike the behavior of the powder material, the line shape as a whole does not

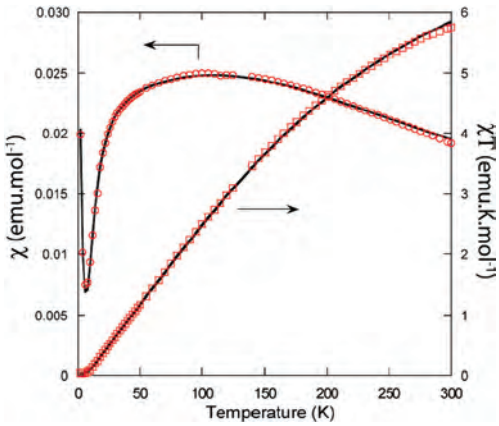

Figure 8. χ (open circles) and χT (open squares) as a function of temperature for **C3**$(MeOH)_2$. Full line corresponds to the fit of the $\chi = f(T)$ curve (text) and to the corresponding χT product.

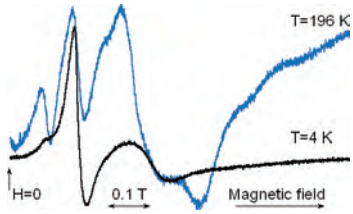

Figure 9. Experimental EPR powder spectra of **C3**$(MeOH)_2$ at 4 and 196 K.

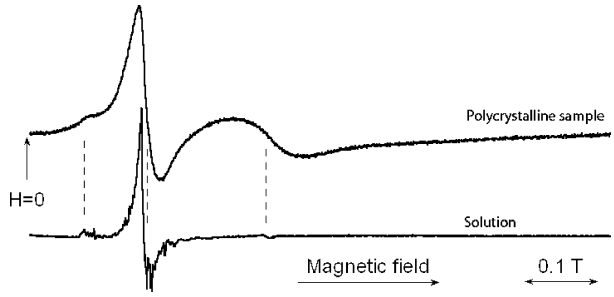

Figure 10. Comparison of some selected experimental EPR spectra of complex **C3** in polycrystalline form and in frozen solution, at 4 K.

significantly change in solution between 4 and 95 K. This signal must be attributed to isolated high-spin hexacoordinated Fe^{III} ions resulting from the decoupling of the Fe−Fe dimer, as observed in the solid state, that is, it corresponds to the separation of the dimer complex in solution. This is evidenced by the actual similarity of the spectra recorded for the dimer in solution and for a monomer prepared with a closely related ligand (Figure S6 in the Supporting Information).

As a summary, the EPR spectra in the solid state correspond to a magnetic behavior parallel to the one observed by SQUID. Moreover, the studies in solution point to the decomplexation of the dimer units, resulting in monomer units. Such unreacted monomers are probably responsible for the Curie tail in the SQUID susceptibility and of the EPR signal of the powder at 4 K.

Electrochemical Studies of the C1 and C2 Iron Complexes. C1 has been investigated by cyclic voltammetry as well as pseudosteady state voltammetry. In Figure 11 are gathered cyclic voltammograms measured on **C1** as well as H_2L ligand (in insert). In both cases, the presence of ferrocene

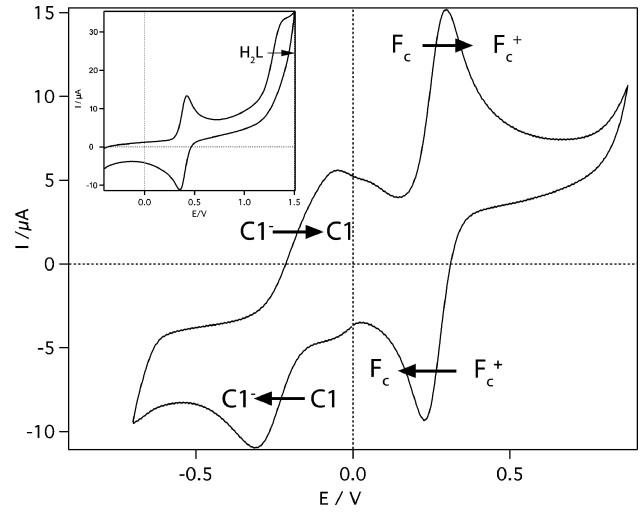

Figure 11. Cyclic voltammogram of **C1** (1 mM) in DMF at a platinum electrode, supporting electrolyte 0.2 M nBU_4PF_6, scan rate 100 $mV \cdot s^{-1}$, ferrocene as internal standard. Insert, in the same conditions, cyclic voltammogram of the H_2L ligand.

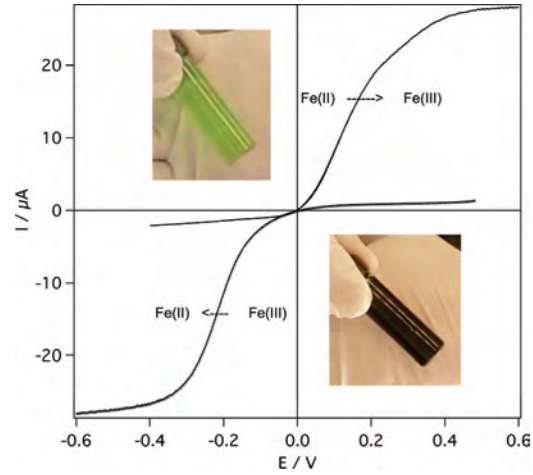

Figure 12. Quasi-steady-state current−potential curves measured on both **C1** (1 mM) and **C2** (1 mM) complexes in DMF at glassy carbon electrode, supporting electrolyte 0.2 M nBU_4NPF_6, scan rate 2 $mV \cdot s^{-1}$, rotation rate: 1000 rpm.

in the mixture indicates the viability of these electrochemical measurements. The **C1** electrochemical signature is in agreement with a reversible **C1/C1**$^-$ system, whereas the H_2L ligand only exhibits the oxidation part of the electrochemical redox cycle. Considering the quasi-steady voltammograms (Figure 12) measured on both **C1** and **C2** complexes, we assume that the **C1/C1**$^-$ electrochemical signal observed in the cyclic voltammogram corresponds to the redox system **C1/C2**. In fact, Figure 12 clearly shows both oxidation and reduction waves of **C2** (yellow solution in DMF) and **C1** (dark blue solution in DMF) complexes, respectively.

In summary, the electrochemical study is consistent with the fact that the color change from blue to yellow during the crystallization process corresponds to the reduction of Fe^{III} to Fe^{II}, that is, a reduction of **C1** to **C2** in solution.

(21) Walker, F-A. *Chem. Rev.* **2004**, *104*, 589.

Conclusions

We have reported the synthesis, structures, and magnetic properties of some new Fe^{III} and Fe^{II} complexes, which illustrate the very rich coordination chemistry of the multidentate hydrazido salicyl derivative ligands bearing sulfur groups. From a synthetic point of view, we have demonstrated that the reaction of 2-salicylichydrazono-1,3-dithiolane ligand (H_2L) with iron (+III) chloride and/or acetylacetonate salts readily affords new monomeric complexes as well as μ-methoxo binuclear complexes in good yields. All new complexes have been fully characterized by single-crystal X-ray diffraction.

Three important results should be highlighted:

• Thanks to EPR studies, this work demonstrates that the Fe^{III} μ-methoxo binuclear complex exists in the crystalline solid state but not in THF solution. This observation seems to indicate that the CH$-\pi$ hydrogen bonds, as clearly detected by single-crystal diffraction, is a key parameter for the stability of the binuclear asymmetric complex. It is is very likely that these hydrogen bonds are broken in THF and/or DMF solvents. This knowledge is crucial for further investigations with such potential magnetic species. Our aim is now to stabilize such μ-methoxo binuclear complexes in solution by specific functionalization.

• The second important result concerns the predicted antiferromagnetic behavior observed for the $Fe^{III}_2(HL)_4(\mu\text{-}OCH_3)_2$ complex in the crystalline solid state. This behavior is completely in line with the orbital model proposed for the analogous ferromagnetic $Mn^{III}_2(HL)_4(\mu\text{-}OCH_3)_2$ complex.[12]

• The third highly relevant observation is the spontaneous reduction of **C1** (Fe^{III}) to complex **C2** (Fe^{II}). The reduction process remains unclear to us but both the electrochemical studies and crystal structure determinations of many **C2** complexes clearly show that the reduction ($Fe^{III} \rightarrow Fe^{II}$) occurs during the crystallization process. It constitutes, to the best of our knowledge, the first example of spontaneous reduction of a high-spin Fe(III) complex in solution to a high-spin Fe(II) complex in solution as well as in the crystalline solid state. Great attention will be focused in this very exciting phenomenon, which opens a very broad spectrum of new opportunities for further investigations. We presently work on Cr^{III}, Co^{III}, and Co^{II} chemistry as well as on specific modifications of the ligands to tune and better understand the intramolecular hydrogen bonds in binuclear compounds.

Experimental Section

All manipulations were performed under aerobic conditions using commercial reagents and solvents.

1. Ligand H_2L. This ligand was prepared as previously described.[13,14]

2. $Fe(HL)_2(DMF)(Cl)$. C1. To a well-stirred solution of H_2L in DMF (64.5 mg, 0.3 mmol in 2 mL) was added $FeCl_3$ (13.7 mg, 0.1 mmol), after 5 h of stirring at room temperature, 8 mL of diethyl ether were added carefully on the surface of the dark solution which was then left undisturbed for slow precipitation (2 to 3 days). The resulting dark crystals of the titled complex were collected by filtration and washed with diethyl ether. (Yield: 35 mg, 62%). Anal. Calcd for $C_{23}H_{25}N_5O_5S_4ClFe$: C, 41.17; H, 3.76; N, 10.44. Found: C, 40.78; H, 4.08; N, 10.56.

3. $Fe(H_2L)_2(Cl)_2$. C2. A yellow solution of $FeCl_3$ (19 mg, 0.12 mmol) in DMF (1 mL) is added to a well stirred colorless solution of the ligand (60 mg, 0.24 mmol) in DMF (2 mL). The color changes immediately from yellow to dark blue. The homogeneous mixture was left under stirring overnight at room temperature. A yellow solution and, when the diffusion process is ended, crystalline powder of the titled complex were obtained after a slow diffusion (2 to 3 days) of diethyl ether into the crude reaction mixture in a sealed glass tube (Yield: 52 mg, 70%). Anal. Calcd for $C_{20}H_{20}N_4O_4S_4Cl_2Fe$ (0.8 Et_2O): C, 40.09; H, 4.05; N, 8.06. Found: C 39.71; H, 4.04; N, 7.67.

4. $Fe_2(HL)_4(\mu\text{-}OCH_3)_2$. C3. This complex can be synthesized by two ways. Starting from $Fe(acac)_3$, a solution of this salt (0.1 mmol 35.5 mg in 2 mL of DMF) was added to a well stirred solution of H_2L (0.2 mmol, 50.8 mg in 2 mL of DMF), and the resulting mixture color changes quickly from colorless to dark brown. The product of this step (typically the mononuclear species) was extracted by THF to yield a dark solution; slow diffusion of methanol into this solution (during 6 to 12 h) affords well-formed dark-red crystals of the titled complex with good yield (45 mg, 73%). Anal. Calcd for $C_{42}H_{42}N_8O_{10}S_8Fe_2$ (1•MeOH): C, 41.30; H, 3.45; N, 9.19. Found: C, 40.98; H, 3.75, N, 9.32. IR (KBr, cm^{-1}): 3513, 2814, 2921, 1619, 1588, 1520, 1487, 1364, 1252. **C3** can also be prepared starting from $FeCl_3$ salt in one step, by reacting (0.2 mmol) of H_2L with (0.1 mmol) of $FeCl_3$ in methanol in the presence of sodium acetate (NaOAc). The recrystallization from THF by slow diffusion of methanol yields well-formed crystals of the complex.

5. Magnetic Measurements. Magnetic measurements were performed at the Institut de Physique et Chimie des Matériaux de Strasbourg (UMR CNRS-ULP 7504) using a Quantum Design MPMS-XL SQUID magnetometer. The susceptibility measurement was performed in the 300−1.8 K temperature range with an applied field of 5 kOe. Magnetization measurements at different fields at room temperature confirm the absence of ferromagnetic impurities. Data were corrected for the sample holder and diamagnetism was estimated from Pascal constants.

6. EPR Measurements. The EPR spectra have been recorded at X-band (ca. 9.8 GHz) with an ESP-300E spectrometer (Bruker) equipped with a rectangular TE 102 cavity and an ESR 900 continuous flow cryostat for liquid helium circulation (Oxford). The static field was controlled with a Hall probe, whereas the microwave frequency was simultaneously recorded with a frequency counter (HP-5350 B). Dilute solutions (ca. 10^{-3} mol) were degassed with argon before recording the spectra.

7. Electrochemistry. Dimethylformamide (DMF) was used as solvent. Before used, DMF was in contact with molecular sieves for 12 h. Tetrabuthylammonium hexafluorophosphate; nBU_4NPF_6 (Fluka, electrochemical grade) was used as supporting electrolyte. All electrochemical measurements were carried out at ambient temperature (20 ± 2 °C) in a classical one compartment three electrodes cell. The working electrodes were platinum electrode (2 mm diameter) or a rotating-disk glassy-carbon electrode (3 mm diameter), the counter electrode was a platinum wire, and a second platinum wire was used as pseudo reference. The cell was connected to a PGSTAT 20 potentiostat (Eco Chemie, Holland). The solution was bubbled with argon before measurements.

8. Crystal Structure Determinations. Single crystals of **C1**, **C2**(Et_2O), **C2**($MeOH)_2$, **C2**($CH_2Cl_2)_2$, and **C3**($MeOH)_2$ were mounted on a Nonius Kappa-CCD area detector diffractometer (Mo Kα λ

= 0.71073 Å). The complete conditions of data collection (*Denzo* software[22]) and structure refinements are given in Table S1 in the Supporting Information. The cell parameters were determined from reflections taken from one set of 10 frames (1.0° steps in phi angle), each at 20 s exposure. The structures were solved using direct methods (*SHELXS97*) and refined against F^2 using the *SHELXL97* and *CRYSTALBUILDER* softwares.[23,24] The absorption was not corrected. All non-hydrogen atoms were refined anisotropically. Hydrogen atoms were generated according to stereochemistry and refined using a riding model in *SHELXL97*. Crystallographic data (excluding structure factors) have been deposited in the Cambridge Crystallographic Data Centre as Supplementary publication no. CCDC 679931−679933, 682062, 682063. Copies of the data can be obtained free of charge on application to CCDC, 12 Union Road, Cambridge CB2 1EZ, UK (fax: (+44)1223−336−033; e-mail: deposit@ccdc.cam.ac.uk).

Acknowledgment. We thank the CNRS and the Ministère de la Recherche (Paris) for the Ph.D. grant of Nicolas Clément and the Agence Nationale de la Recherche (ANR contract no. ANR-06-JCJC-0008) for funding. We also thank Dr. Pierre Braunstein and Dr. Dominique Mandon for fruitful discussions.

Supporting Information Available: Fully labeled *ORTEP* views; figures of $1/\chi = f(T)$ plot for complex C2, Et2O, and additional experimental EPR spectra; CIFs; and tables of crystal data and X-ray structure refinement parameters at 173 K for all complexes. Hydrogen bonds detected in the crystal structures of C1, [C2, Et_2O], [C2,$(MeOH)_2$], [C2,$(CH_2Cl_2)_2$], and [C3,$(MeOH)_2$]. This material is available free of charge via the Internet at http://pubs.acs.org.

IC800522H

(22) *Kappa CCD Operation Manual*, Nonius B. V., Ed.; Delft: The Netherlands, 1997.
(23) Sheldrick, G-M., *SHELXL97, Program for the Refinement of Crystal Structures*; University of Göttingen: Göttingen, Germany, 1997.
(24) Welter, R. *Acta Crystallogr.* **2006**, *A62*, s252, The Crystalbuilder Project.